AFRL-AFOSR-JP-TR-2016-0056

Multi-Ferroic Polymer Nanoparticle Composites for Next Generation Metamaterials

Yuanzhe Piao
SEOUL NATIONAL UNIVERSITY
SNUR&DB FOUNDATION RESEARCH PARK CENTER
SEOUL, 151742
KR

05/23/2016
Final Report

Air Force Research Laboratory
Air Force Office of Scientific Research
Asian Office of Aerospace Research and Development
Unit 45002, APO AP 96338-5002

REPORT DOCUMENTATION PAGE

Form Approved
OMB No. 0704-0188

1. REPORT DATE *(DD-MM-YYYY)*	2. REPORT TYPE	3. DATES COVERED *(From - To)*
23-05-2016	Final	30 Mar 2012 to 29 Mar 2015

4. TITLE AND SUBTITLE
Multi-Ferroic Polymer Nanoparticle Composites for Next Generation Metamaterials

5a. CONTRACT NUMBER
FA2386-12-1-4015

5b. GRANT NUMBER
Grant 12IOA075_124015

5c. PROGRAM ELEMENT NUMBER
61102F

6. AUTHOR(S)
Yuanzhe Piao

5d. PROJECT NUMBER

5e. TASK NUMBER

5f. WORK UNIT NUMBER

7. PERFORMING ORGANIZATION NAME(S) AND ADDRESS(ES)
SEOUL NATIONAL UNIVERSITY
SNUR&DB FOUNDATION RESEARCH PARK CENTER
SEOUL, 151742 KR

8. PERFORMING ORGANIZATION REPORT NUMBER

9. SPONSORING/MONITORING AGENCY NAME(S) AND ADDRESS(ES)
AOARD
UNIT 45002
APO AP 96338-5002

10. SPONSOR/MONITOR'S ACRONYM(S)
AFRL/AFOSR/IOA(AOARD)

11. SPONSOR/MONITOR'S REPORT NUMBER(S)
12IOA075_124015

12. DISTRIBUTION/AVAILABILITY STATEMENT
Distribution Code A: Approved for public release, distribution is unlimited.

13. SUPPLEMENTARY NOTES

14. ABSTRACT
The purpose of this research project is to develop magnetodielectric polymer composites consisting of magnetic nanoparticles that possess high , and low tan and polymer matrix with high dielectric constant and permeability. Particularly for Microwave communication devices high dielectric constant (), permittivity () and permeability and low dielectric loss (tan) is highly desired. To accomplish the goal magnetic nanoparticles in polymer matrix are investigated including uniform distribution of nanoparticles and characterization of size dependence of nanoparticles. The work is collaborated between Seoul National University, Korea and University of Maryland.

15. SUBJECT TERMS
Magnetoresistance, Metamaterials, Nanocomposites, Nanoparticles

16. SECURITY CLASSIFICATION OF:			17. LIMITATION OF ABSTRACT	18. NUMBER OF PAGES	19a. NAME OF RESPONSIBLE PERSON
a. REPORT	b. ABSTRACT	c. THIS PAGE			MAH, MISOON
Unclassified	Unclassified	Unclassified	SAR	13	19b. TELEPHONE NUMBER *(Include area code)* 042-511-2001

Standard Form 298 (Rev. 8/98)
Prescribed by ANSI Std. Z39.18

Multi-Ferroic Polymer Nanoparticle Composites for Next Generation Metamaterials

AOARD

Final Report

April 25th 2016

Yuanzhe Piao, Seoul National University, Korea, parkat9@snu.ac.kr

Introduction

For microwave communications devices, high dielectric constant (μ), permittivity (ε) and permeability and low dielectric loss (tan δ) is highly desired. In order to actualize materials having such properties, magnetic nanoparticles in polymer matrix is a very good option since it has high μ and ε along with high dielectric constant and mechanical elasticity. Thus the purpose of this research project is to develop magnetodielectric polymer composites consisting of magnetic nanoparticles that possess high μ, ε and low tan δ and polymer matrix with high dielectric constant and permeability. In order to endow magnetic nanoparticles having high permeability with high dielectric constant, polymers have been used[1,2]. However, it is very hard to achieve such materials possessing high dielectric constant and low loss[3]. Inorganic magnetic nanoparticles in polymer matrix system requires uniformly distributed nanoparticles for the application. But uniform distribution cannot be easily achieved due to strong van der waals interaction between nanoaparticles which induces them to aggregate[3]. Moreover, depends on the size and shape of magnetic nanoparticles, the magnetic properties can vary. So it is very important to synthesize the uniform and monodisperse magnetic nanoparticles.

So, we, as a team of this collaboration project, focused on synthesizing uniform and monodisperse magnetic nanoparticles. First, we synthesized silica-coated monodisperse iron oxide nanoparticles (≈ 30 nm) sent to University at Maryland for further step, magnetodielectric measurement. Silica-coated uniform iron oxide nanoparticles can be uniformly distributed in a PDMS matrix and this is used for comparison for the other work. Beside, conductivity along with other properties we discussed above is a key issue for another application, electromagnetic wave shielding. Electromagnetic wave induces current which results in loss of energy. Thus magnetic nanoparticles should stay in conductive matrix. We synthesized ordered iron oxide nanoparticles in carbon sheet using a salt. We also developed a new synthetic method for uniform and monodisperse iron oxide nanoaparticles on conductive graphene sheets. This novel method is solventless and very simple but the result is remarkable.

Magnetite/silica core-shell nanoparticles for flexible magnetodielectric composites

Composites with magnetite nanostructures fillers invented by the other team member, Professor. Kofinas, demonstrated extraordinary magnetodielectric qualities. For purpose of comparison, this work was done. Conventional magnetite nanoparticles in a PDMS matrix were examined by high frequency magnetodielectric measurements. We synthesized monodisperse magnetite nanoparticles using a thermal decomposition method. Silica coating was done by reverse microemulsion. Silica layers on magnetite nanoparticles minimize the surface tension between the PDMS polymer matrix and magnetite nanoparticles, which results in better dispersion in the PDMS matrix. In **Figure 1**, uniform monodisperse silica-coated magnetite nanoparticles are shown. The average size is ≈ 30 nm and the thickness of silica layer is ≈ 12 nm.

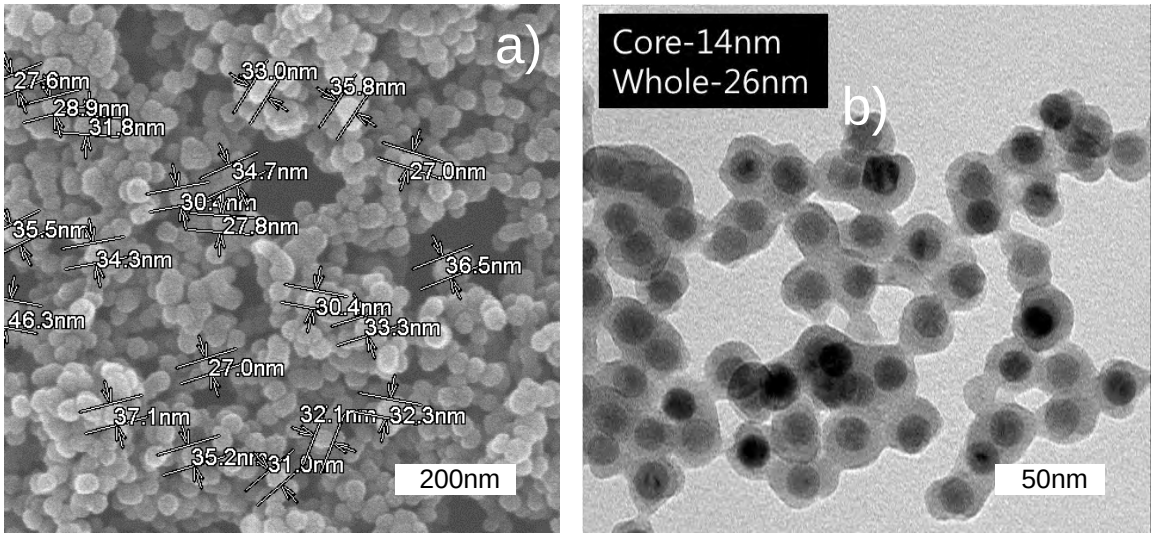

Figure 1. a) Scanning electron microscopy (SEM) images of magnetite-silica core shell nanoparticles. b) Transmission electron microscopy (TEM) images of magnetite-silica core shell nanoparticles.

Two samples (thin and thick silica shell) were prepared. Both thin silica shell (3 nm) sample and thick silica shell (12 nm) sample was synthesized by controlling Tetraethyl orthosilicate (TEOS) and ammonia solution concentration. The composites were used as nanoparticles fillers in the PDMS matrix. The composites impregnated in the PDMS polymer. The polymer matrix was cured by heat. Thin and thick silica shell samples were mixed with PDMS polymer by 20wt% and 50wt%, accordingly. These concentrations are reported as the highest achievable concentrations using simple mixing of particles with the polymer matrix before curing.

Due to the weight of silica shell in the composites, the permittivity values of the composites were relatively lower than that of conventional magnetite nanoaparticles[4,5,6] (**Figure 2**).

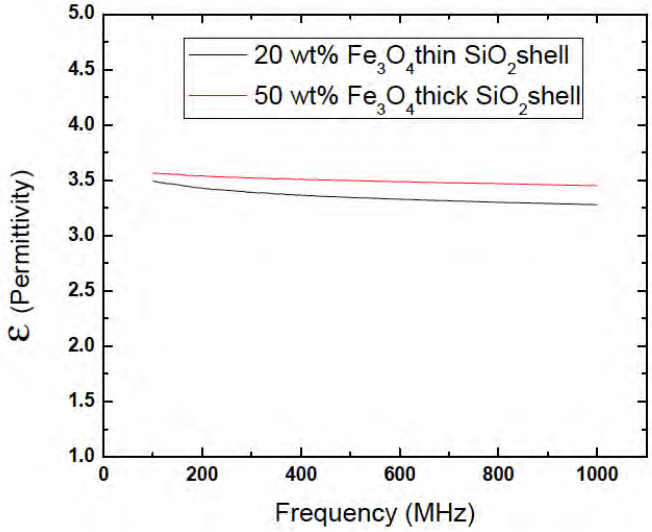

Figure 2. Permittivity (ε) for composites with core-shell nanoparticles of magnetite-silica

The dielectric loss of the thick silica shell composite is relatively lower than that of the thin silica shell composite. This is because of the insulating silica layer and polymer matrix (**Figure 3**)

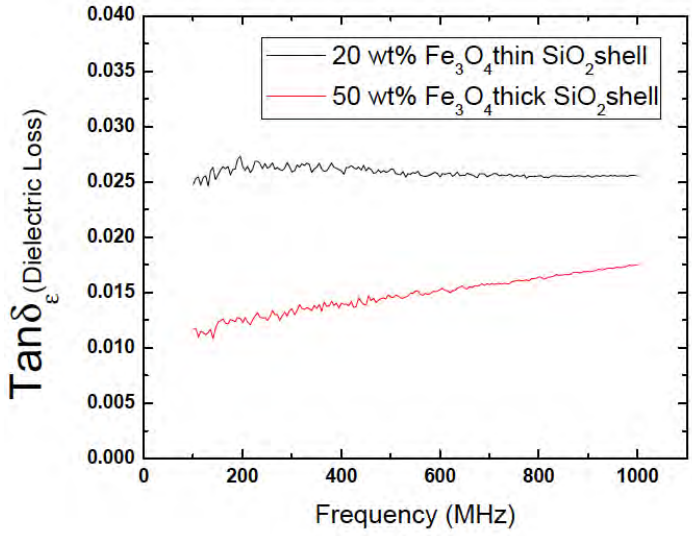

Figure 3. Dielectric loss (tan δ) for composites with core-shell nanoparticles of magnetite-silica

Permeability (μ) of both samples are presented in **Figure 4**. The thick silica coated magnetite nanoparticle sample exhibits low permeability values of 1.12 at 1 GHz with 50 wt% high loading. Due to Snoek's limit which implies the more increase permeability, the more increase magnetic loss values, the magnetic loss values of the composites are higher when the low permeability values are taken into account.

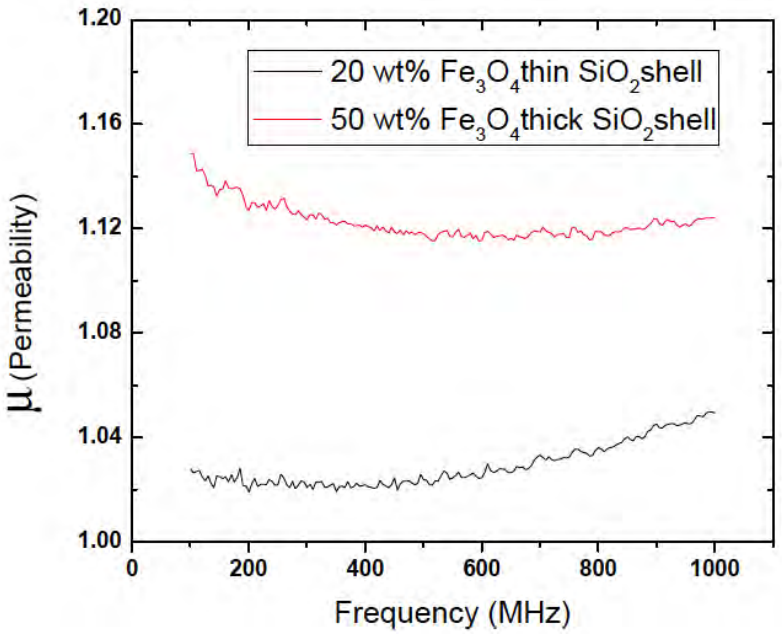

Figure 4. Permeability (μ) of composites with core-shell nanoparticles of magnetite-silica

Since the permeability of the conventional magnetite based polymer composites decays rapidly with increasing the frequency beyond their resonance ranges, the operating frequencies are limited (< 1 GHz). The magnetite-silica composites also exhibit the similar results. Less than 1 GHz resonance frequency is not beneficial for magnetodielectric composites. Even if silica shell keeps low dielectric loss by silica layers acting as insulating layer giving the magnetite nanoparticles to decreased electric conductivity which prevents induced electricity from being generated, it hinders the magnetic contribution of the magnetite. This leads to low overall permeability. This final results give good comparison to the other work done by Professor. Kofinas.

A novel synthetic method of ordered iron oxide nanoparticles on carbon nanosheets

Ordered iron oxide nanoparticles assembled on carbon nanosheet can be potentially applicable for electromagnetic wave shielding. For better electromagnetic wave shielding capability, i) high dielectric constant, ii) high magnetic permeability and iii) high electric conductivity are required. Moreover, it is known that two dimensional structure can exhibit the excellent electromagnetic wave shielding properties[7,8]. In such point of view, designing a structure, magnetic nanoparticles in two dimensional electric conductive matrix, is possible approach.

Two dimensional nanostructures of ferrite/carbon composites were directly synthesized from metal-oleate precursor through a salt-template process. The metal-oleate precursor could be made by mixing metal chloride and sodium oleate in ethanol, hexane and D.I. water. Detailed synthesis scheme is below (**Figure 5**).

Figure 5. The overall scheme for the metal-oleate complex. (*Nature Materials* 2004,**3**, 891)

Following this scheme, iron-oleate complex were synthesized by mixing iron chloride and sodium oleate in solvents. NaCl, byproduct of iron-oleate could be eliminated by extraction process. The synthesized iron oleate mixed with sodium sulfate powder as a sacrifice template and then heated to 600 °C at the heating rate of 10 °C. During heating process, carbon layer was formed due to the carbonization of oleate. Finally, 16 nm iron-oxide/carbon sheet hybrid nanosheets were formed. A single-step method for the direct preparation of self- assembled ferrite/carbon hybrid nanosheets is presented below (**Figure 6**).

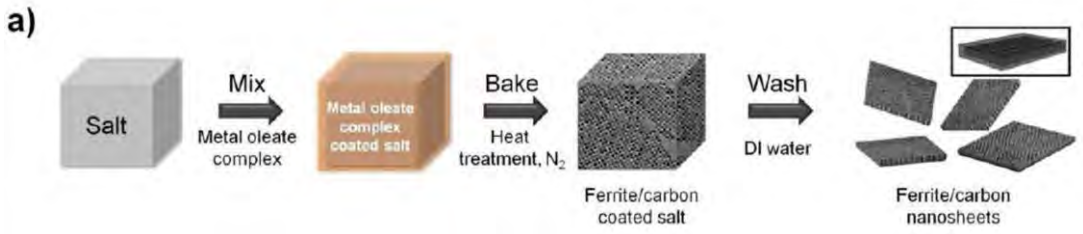

Figure 6. (a) Schematic representation of the preparation of ferrite/carbon nanosheets by salt-template process

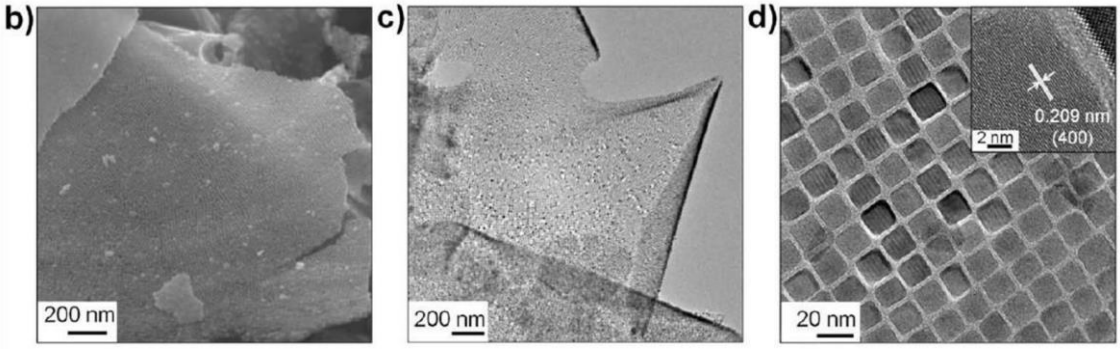

Figure 7. (b) FE-SEM image (c,d) TEM images of 16nm of iron-oxide carbon / nanosheets The inset shows a HR-TEM image demonstrating the highly crystalline nature of the nanosheets.

FE-SEM image (**Figure 7**a) shows that a well-ordered iron oxide nanoparticles were embedded in a carbon sheet with long-range ordered arrays. The shape of iron oxide nanoparticles is cubic type (Figure 7b) and the nanocubes were highly crystalline with d-spacing of the lattice fringes indicate that the faces of the nanocubes are {100} planes (Figure 7c). The evolution of the cubic shape is attributed to the relative stabilization of the {100} face as compared to the {111} and {110} faces.

The size and shape of iron oxide nanoparticles could be controlled by changing the heating rate.

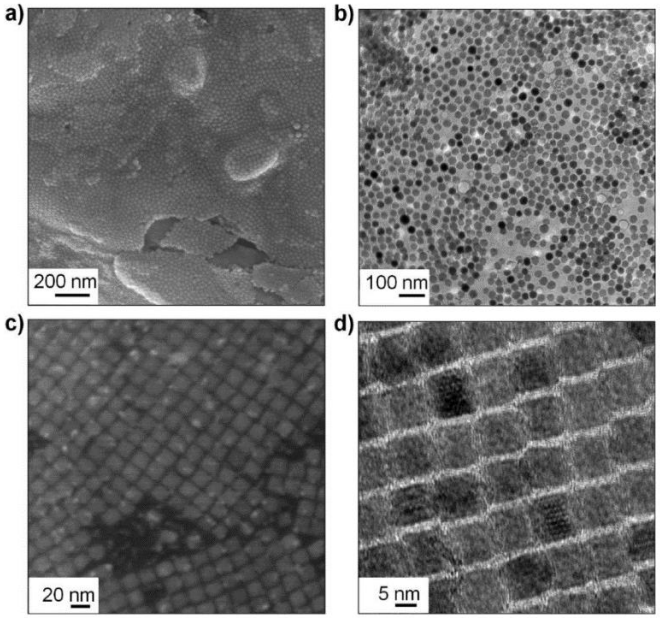

Figure 8. (a) FE-SEM image and (b) TEM image of 30 nm iron-oxide/carbon nanosheets, (c) FESEM image and (d) TEM image of 10nm manganese-ferrite /carbon nanosheets.

30 nm spherical iron oxide nanoparticles could be synthesized (**Figure 8**a,b) when the heating rate was 5 °C min^{-1} as compared to heating rate of 16nm cubic iron oxide nanoparticles was 10 °C min^{-1}.

Even manganese ferrite nanoparticles could be substitute instead of iron oxide nanoparticles.

Manganese ferrite nanoparticles could be embedded in to carbon layer (Figure 8c) and homogeneous manganese ferrite could be formed (Figure 8d).

In addition hollow carbon layer could be formed by eliminating metal oxide nanoparticles using HNO_3 solution. (Figure 9a)

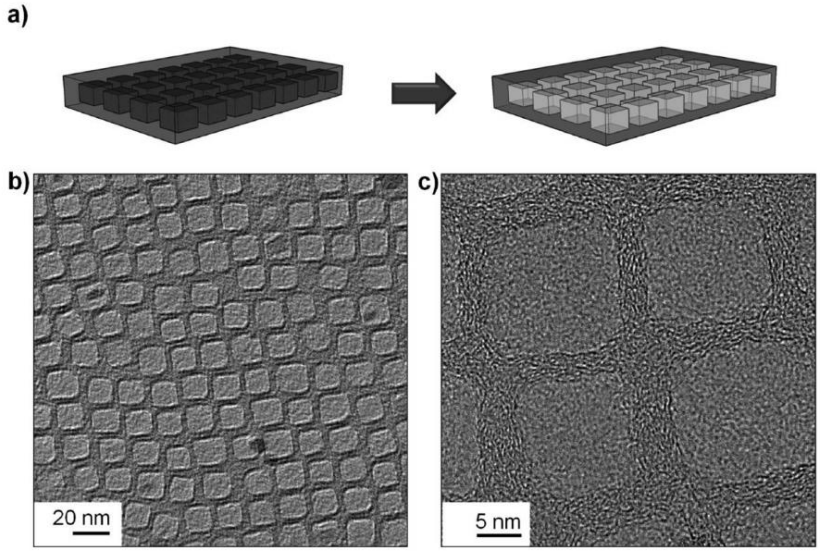

Figure 9. (a) Synthetic scheme of hollow carbon layer (b,c) TEM images of carbon nanofoams after removal of 16nm iron oxide nanocrystals from the nanosheets.

Hollow carbon nanofoams could be formed using acid solution (**Figure 9**b,c)

In conclusion, we synthesized metal-oxide/carbon nanosheets which potentially can be applicable for electromagnetic wave shielding. The structure of ordered iron oxide nanoparticles on carbon nanosheets can be expected to show good electromagnetic wave shielding properties due to uniform and monodisperse iron oxide nanoparticles on two dimensional conductive carbon nanosheets.

Solventless synthesis of magnetite/graphene nanocomposite

There have been a lot of interests in electromagnetic wave shielding effect using hybrid nanocomposite which is comprised of inorganic materials and carbon substrates[9]. When the incident EM wave is irradiated to such nanocomposite, the light can be either reflected, scattered or absorbed due to the multiplexed structure of dielectric inorganic nanocrystals and graphene layers, even enhance the inter-layered effect (**Figure 10**). Especially, graphene with its two dimensional nature has exhibited the excellent electromagnetic wave shielding performance[10,11,12,13].

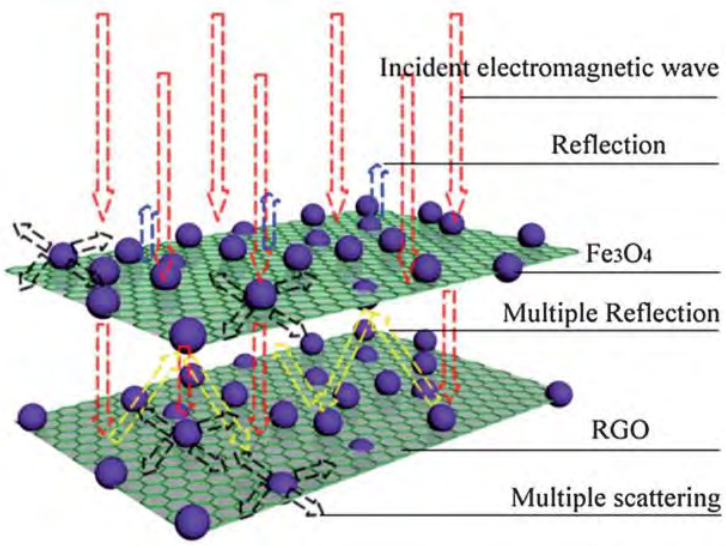

Figure 10. Illustration of possible microwave absorption mechanisms in graphene/magnetite nanocomposites (*J. Mater. Chem. C*, 2013, **1**, 765)

In this research, we focused on the synthesis of iron oxide nanoparticles which have uniform size and shape and directly grown on graphene sheets. Previously reported papers showed surfactant-mediated assembly of ready-made nanoparticles and graphene sheets, however they suffered several problems due to the residual surfactants and low production yields. Thus we developed the direct thermal decomposition of iron containing precursors on reduced graphene sheets. Regarding the synthesis, we mixed the iron acetylacetonate powder and rGO powder with some of oleic acid. Then the mixture was hand-milled to make reddish-black slurry and baked at 600℃ under inert atmosphere.

Regarding the synthesis, the method in this research realized a very handy synthesis with less complicated preparations. Previous researches synthesized iron oleate complex prior to use and it takes a day to get rid of residual salts. Thus we substituted the complicated process to simple mixing of iron acetylacetonate and oleic acid. In case of the graphene nanocomposite, the formation was achieved via single step thermal decomposition which saves a lot of time and consumes less expenses.

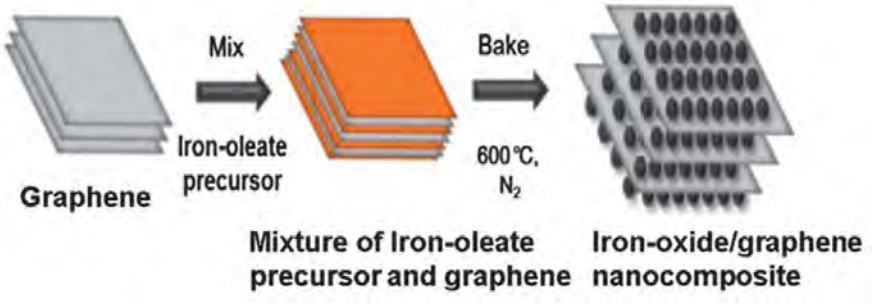

Figure 11. Comprehensive drawings of iron oxide/graphene nanocomposite synthesis

After the heat treatment, resultant black powder was investigated through transmission electron microscopy and scanning electron microscopy in order to confirm its morphological properties. The synthesized magnetite nanocrystals were sized about 20nm and they were firmly loaded onto the layered rGO sheets. Also we conducted thermogravimetric analysis for understanding the loaded mass of magnetite and it was about 32 wt.%.

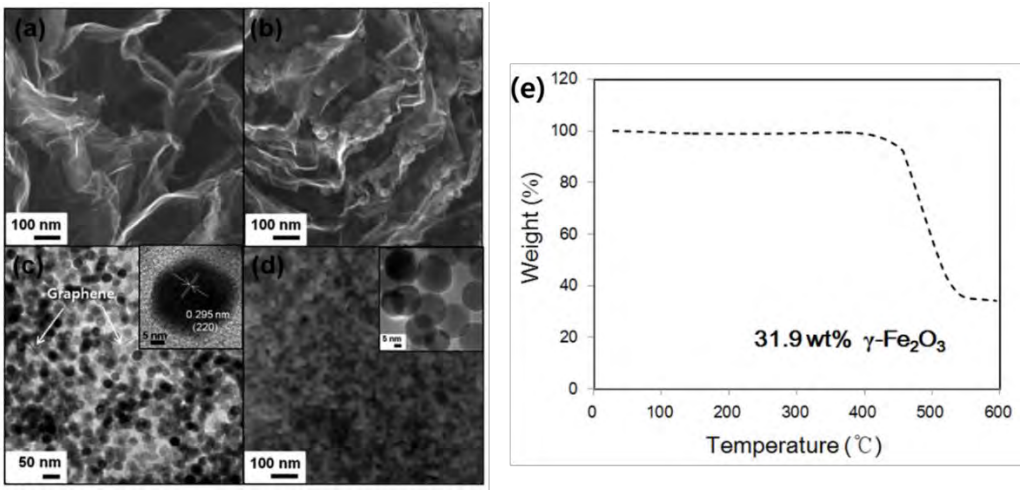

Figure 12. (a) FE-SEM image of the as-prepared graphene, (b) FE-SEM image and (c) TEM image of the iron-oxide/graphene nanocomposite and (d) SEM image of the iron oxide nanoparticle. The inset figure represents a high resolution TEM image of the iron oxide nanoparticle. (e) TGA analysis of iron oxide/graphene nanocomposite

After the structural confirmation, we also investigated the materials phase via X-ray diffraction analysis. The as-made iron oxide showed mixed phase of hematite and maghematite, however, due to the surface interaction between the reduced graphene sheet and iron ions, synthesized magnetic nanoparticles only showed maghemite curves in nanocomposites.

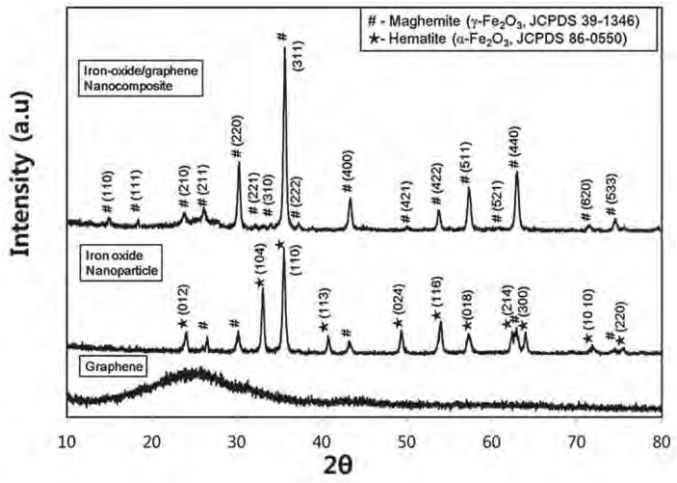

Figure 13. X-ray diffraction analysis of as made iron oxide/graphene nanocomposite

We expect, the synthesized nanocomposite is under further post-process for electromagnetic wave shielding measurement and its multi-layered hybrid is highly expected in electromagnetic wave-related applications because of its good electric conductivity and uniform and monodispersed magnetic nanoparticles.

Conclusion

We demonstrated magnetite/silica core-shell nanoparticles for flexible magneto-dielectric composites and two novel synthetic methods for potentially applicable electromagnetic wave shielding materials. Silica shells on magnetite nanoparticles provide well dispersion in the PDMS matrix which enhances magnetodielectric properties. Since it was synthesized as a control group, it showed reasonable performances. We also proposed the structure of ordered iron oxide nanoparticles on carbon nanosheets, because three properties, high dielectric constant, high permeability and high electric conductivity, are necessary for good electromagnetic wave shielding materials. We expect, this uniform and well dispersed magnetic nanoparticles on two dimensional conductive structure will show the good electromagnetic wave shielding performance. Graphene is being widely studied and also has the excellent electromagnetic wave shielding performance due to its two dimensional nature and high electric conductivity. We synthesized well-dispersed uniform magnetic nanoparticles on graphene nanosheets by a facile solventless method. Simple mixing and heating is enough for this novel structures. We strongly believe, this material also will show the excellent electromagnetic wave shielding performance.

References

1. Q. Wang, L. Zhu, *J. Polym. Sci., Part B: Polym. Phys.* 2011, **49**, 1421-1429.

2. Z.-M. Dang, J.–K. Yuan, S.–H. Yao, R.–J. Liao. *Adv. Mater.* 2013, **25**, 6334-6365.

3. L. Zhu, *J. Phy. Chem. Lett.* 2014, **5**, 3677-3687.

4. T. I. Yang, R. N. C. Brown, L. C. Kempel and P. Kofinas, *J. Magn. Magn. Mater*, 2008, **320**, 2714-2720.

5. S. H. Park, W. K. Ahn, J. S. Kum, J. K. Ji, K. H. Kim and W. M. Seong, *Electron Mater Lett*, 2009, **5**, 67-71.

6. A. Caprile, M. Coisson, F. Fiorillo, P. Kabos, O. M. Manu, E. S. Olivetti, M. A. Olariu, M. Pasquale and V. A. Scarlatache, *Ieee T Magn*, 2012, **48**, 3394-3397.

7. H. B. Zhang, Q. Yan, W. G. Zheng, Z. X. He and Z. Z. Yu, ACS *Appl. Mater. Interfaces*, 2011, **3**(3), 918–924.

8. J. J. Liang, Y. Wang, Y. Huang, Y. F. Ma, Z. F. Liu, J. M. Cai, C. D. Zhang, H. J. Gao and Y. S. Chen, *Carbon*, 2009, **47**, 922–925.

9. F. Shahzad, P. Kumar, S. Yu, S. Lee, Y.-H. Kim, S. M. Hong, C. M. Koo, *J. Mater. Chem. C*, 2015, **3**, 9802-9810.

10. C. Wang, X. J. Han, P. Xu, X. L. Zhang, Y. C. Du, S. R. Hu, J. Y. Wang and X. H. Wang, *Appl. Phys. Lett*., 2011, **98**, 072906.

11. X. Bai, Y. H. Zhai and Y. Zhang, *J. Phys. Chem. C*, 2011, **115**, 11673–11677.

12. V. K. Singh, A. Shukla, M. K. Patra, L. Saini, R. K. Jani, S. R. Vadera and N. Kumar, *Carbon*, 2012, **50**, 2202–2208.

13. X. Sun, J. He, G. Li, J. T. Tang, T. Wang, Y. Guo, H. Xue. *J. Mater. Chem. C*, 2013, **1**, 765-777